Cosmogenic ^{21}Ne exposure ages on late Pleistocene moraines in Lassen Volcanic National Park, California, USA

Joseph P. Tulenko[1,2], Greg Balco[3,1], Michael A. Clynne[4], L.J. Patrick Muffler[4]

[1]Berkeley Geochronology Center, Berkeley, CA, 94709, USA
[2]Department of Geology, University at Buffalo, Buffalo, NY, 14260, USA
[3]Lawrence Livermore National Laboratory, Livermore, CA, 94550, USA
[4]USGS Volcano Science Center, Moffett Field, CA, 94035, USA

Correspondence to: Joseph P. Tulenko (jtulenko@bgc.org)

Abstract. We report new cosmogenic ^{21}Ne ~~-~~in ~~-~~quartz exposure ages from 18 samples on three distinct moraines deposited in the Lost Creek drainage, approximately 3–7 km down-valley from Lassen Peak in Lassen Volcanic National Park. Although measuring ^{21}Ne in quartz is generally straightforward, accurate ^{21}Ne exposure dating of deposits of late Pleistocene ~~-age~~ is rarely possible due to the significant quantities of non-cosmogenic ^{21}Ne present in most lithologies. Young quartz-bearing volcanic rocks have been observed to be an exception. We take advantage of moraine boulders sourced from the ~28 ka dacite of Lassen Peak to generate a chronology of alpine deglaciation in Lassen Volcanic National Park. Ages from three distinct moraines are in stratigraphic order at 22.1 ± 3.8 ka, 20.2 ± 2.4 ka, and 15.3 ± 3.8 ka~~,~~ ~~ranging ~22–15 ka,~~ and generally agree with other terminal and some recessional moraine ages across the Cascade Ranges~~-~~ and Sierra Nevada ~~-Range~~ of the western United States. To date, these are among the youngest surfaces ever dated using cosmogenic ^{21}Ne and provide a cost-effective proof-of-concept approach to dating moraines where applicable.

1 Introduction

Moraines deposited on the landscape from past alpine glaciers mark the culmination of glacier advances and, when carefully mapped and dated, can record the ~~magnitude~~extent and timing of these advances. One of the most effective tools for dating moraines is cosmogenic-nuclide exposure dating because 1) it provides a direct age constraint on the landform~~,~~, and 2) in many alpine glacier settings, glaciers can be highly erosive. ~~Glacial erosion and transport are important processes that act to both remove cosmogenic nuclides from previously exposed surfaces and expose previously shielded rocks and sediments to the cosmic ray flux at Earth's surface (Balco, 2011).~~ Glacial erosion and transport are important processes that act to remove exposed or partially exposed rock mass containing inherited cosmogenic nuclides from the landscape and thereby expose previously shielded rocks and sediments to the cosmic ray flux at Earth's surface (Balco, 2011). Thus, the inventory of cosmogenic nuclides on the landscape is reset, and the accumulation of new nuclides tracks with the timing of glacier recession and exposure. For late Pleistocene ~~-age~~ glaciations, the common target cosmogenic nuclide has been ^{10}Be for several reasons; 1) it is produced in quartz (which is easily isolated from other minerals and relatively common), 2) its

geologically short half-life (1.386 x 10^6 yr; Chmeleff et al., 2010) limits the amount of background ^{10}Be in fresh rock surfaces, 3) the production of ^{10}Be on Earth is almost exclusively through cosmic radiation (Gosse and Philips, 2001), and 4) it can reliably be measured at low concentrations. However, ^{10}Be analyses require time-consuming wet chemical dissolution under clean lab conditions, and costly analytical measurements via Accelerator Mass Spectrometry. In some cases, other cosmogenic nuclides – particularly noble gas cosmogenic noble gases nuclides like ^{21}Ne and ^{3}He that have higher production rates than ^{10}Be and do not require AMS measurements – can be used as time-saving and cost-effective alternatives.

During glacial periods throughout the late Pleistocene, alpine glaciers and ice caps flowed from numerous high mountain centers in the western United States and deposited detailed sequences of moraines (Palacios et al., 2020). Glacial geologists have extensively dated these moraines in the western US using surface -exposure dating; to date, more than 2100 samples have been analyzed in 85 publications (data pulled from ICE-D, https://www.ice-d.org; last access 09/20/2023; query used to pull data available on request). Moraines deposited during the latest global glacial interval, termed the Last Glacial Maximum (LGM; 26-19 ka, Clark et al., 2009) and subsequent last deglaciation (19-11 ka; Clark et al., 2012) have been thoroughly investigated in several regions in the western US (see Laabs et al., 2020 and references therein). Moraines dated primarily with surface-exposure dating have linked alpine glacial patterns to local and regional climate mechanisms inferred from other climate proxies – including enhanced precipitation inferred from pluvial lakes (Laabs et al., 2009; Quirk et al., 2020), Laurentide Ice Sheet-atmosphere dynamics (Tulenko et al., 2020), and global climate drivers such as atmospheric CO_2 (Shakun et al., 2015). These observations of past glacier advances, and their linkages to climate change, provide important context for current and future climate and glacier change.

The Cascades Volcanic Arc, located on the western North American margin, is the product of active subduction of the Juan de Fuca plate below the North American Plate. The arc hosts numerous volcanoes, and volcanism has been active throughout the Pleistocene and Holocene (O'Hara et al., 2020). The detailed history of the Lassen Volcanic Center (herein the LVC) in nNortheastern California (Figs. 1 and 2) – the southernmost active volcano system in the arc – is well documented (Christiansen et al., 2002; Clynne and Muffler, 2010). The most important volcanic deposit for our study is referred to as the dacite of Lassen Peak (further described below), which is the result of the emplacement of a volcanic dome at 28.3 ± 2.7 ka (^{40}Ar/^{39}Ar age; Turrin et al., 1998). The dome was likely glaciated during the LGM as several drainages flowing radially outward from the LVC contain well-preserved sequences of moraines comprised of till dominated by dacite of Lassen Peak (Fig. 2). For this study, we focus on moraines deposited 3–7 km down-valley on the northern side of Lassen Peak in the Lost Creek drainage (Figs. 2 and 3).

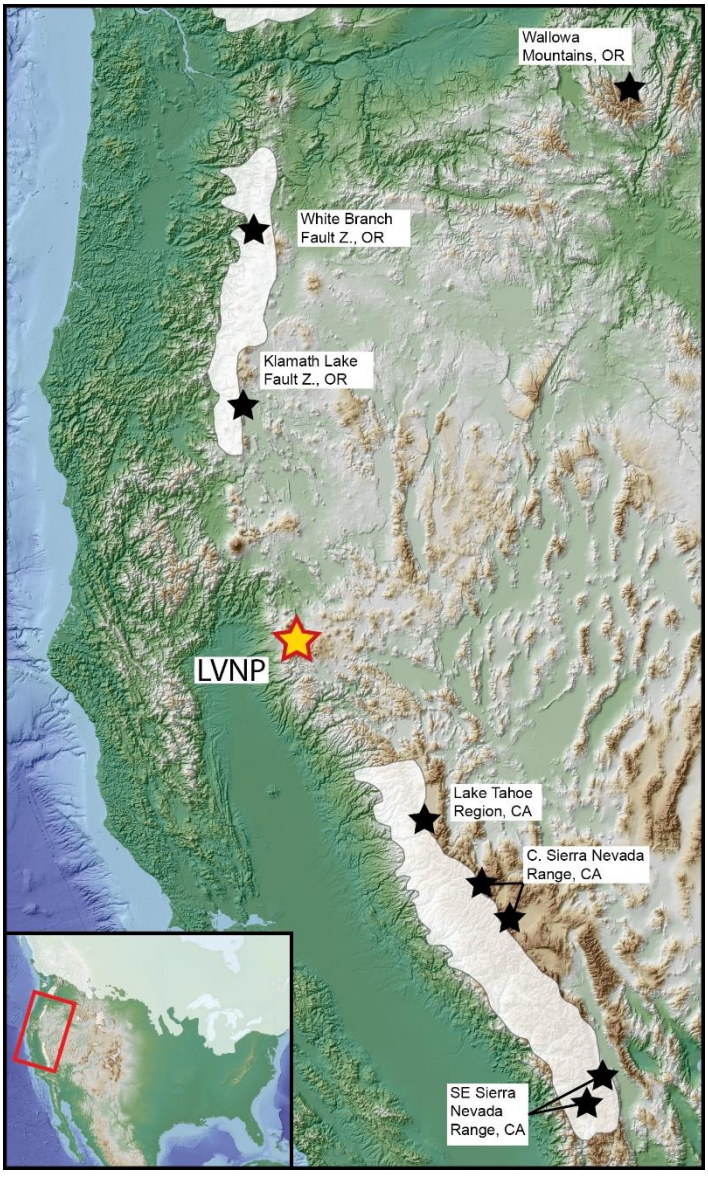

Figure 1. Map of the Cascades Range and Sierra Nevada region with small stars of other previously investigated sites with glacier chronologies. Wallowa Mountains, OR; Licciardi et al., 2004, White Branch Fault Zone; Alexander et al. (2022), Klamath Lake Fault Zone, OR; Speth et al. (2018), Lake Tahoe rRegion, CA; Pierce et al. (2017), central Sierra Nevada Range, CA; Rood et al. (2011a, 2011b), southeast Sierra Nevada Range, CA; Benn et al. (2006), Amos et al. (2010). The large yellow star denotes the location of our study site in Lassen Volcanic National Park. Inset: Map of the US and portions of Canada with overlain limits of LGM glaciation in North America from Dalton et al. (2020) outlined and filled in semi-transparent white polygons.

This paper presents 18 new cosmogenic ^{21}Ne in quartz exposure ages from large boulders situated atop three distinct moraines in the Lost Creek drainage of Lassen Volcanic National Park. Although measurements of cosmogenic ^{21}Ne in quartz by noble gas mass spectrometry are generally straightforward, ^{21}Ne is rarely used for exposure-dating of LGM-age deposits for two reasons. First, neon extracted from quartz is a mixture of atmospheric and in-situ cosmogenic neon (Niedermann 1993, 2002). Although the two are easily distinguished by their distinct isotopic compositions (see section 3.3), the presence of large amounts of atmospheric neon decreases the precision with which the cosmogenic neon inventory can be measured. For example, concentrations of atmospherically derived ^{21}Ne in quartz are commonly in the range 50-100 x 10^6 Matoms/g (Niedermann, 1993, 2002). For a sample with an LGM exposure age and 1 x 10^6 Matoms/g of cosmogenic ^{21}Ne, this means that only 1-2% of the total ^{21}Ne released is cosmogenic; even if the Ne isotope ratios used to deconvolve atmospheric and cosmogenic inventories are measured with 1% precision, this still leads to a 50% uncertainty on the amount of cosmogenic ^{21}Ne. Second, quartz in most lithologies contains significant quantities of nucleogenic neon produced as a byproduct of decay of naturally occurring trace U and Th (Niedermann 2002), which, unlike atmospheric neon, cannot be distinguished from cosmogenic neon using the isotopes of neon (^{20}Ne, ^{21}Ne, and ^{22}Ne). Nucleogenic ^{21}Ne concentrations in quartz of 1-10 x 10^6 Matoms/g are commonly observed in lithologies with cooling ages of more than a few million years (e.g., Balco et al., 2019); at the latitude and altitude of the samples in this study, these concentrations would be equivalent to exposure ages of tens to hundreds of thousands of years. Thus, it is rarely possible to

accurately quantify the amount of cosmogenic ^{21}Ne produced since the LGM in the presence of a commonly substantially larger nucleogenic and atmospheric background. For this reason, cosmogenic ^{21}Ne exposure dating has been most applied to deposits with exposure ages of hundreds of thousands to millions of years (Dunai et al., 2005; Balter-Kenney et al., 2020; Spector and Balco, 2021).

Although accurate ^{21}Ne in quartz exposure-dating of LGM-age samples is difficult in nearly all rocks, young quartz-bearing volcanic rocks can be an exception, in certain cases. Because the concentration of nucleogenic ^{21}Ne scales with the cooling age of the rock, nucleogenic ^{21}Ne concentrations in quartz are expected to be essentially negligible in late Pleistocene volcanics. In addition, quartz in extrusive volcanic rocks has been observed to have low concentrations of included atmospheric neon compared to most rocks (e.g., Phillips et al., 1998; Libarkin et al., 2002; Goethals et al., 2009). ~~Although this observation is largely empirical, it is most likely explained by rapid cooling of eruptive rocks from magmatic temperatures (at which neon is diffusively lost from quartz within minutes) to ambient surface temperatures (at which neon is effectively diffusively immobile).~~ Although this observation is largely empirical and, to our knowledge, not supported by any measurements of quartz-magma partition coefficients, it is most likely explained by rapid cooling of eruptive rocks from magmatic temperatures (at which quartz is diffusively open and noble gases are most likely nearly all partitioned into the magma) to surface temperatures (at which neon is effectively diffusively immobile). In addition, residence of quartz at magmatic temperatures immediately prior to eruption makes the presence of any trapped magmatic neon with unusual isotopic composition extremely unlikely (Niedermann, 2002). Thus, obstacles to ^{21}Ne exposure dating that are present in most lithologies are minimized for quartz in late Pleistocene eruptive volcanics.

For this study, the young age, rapid eruptive nature, and lithology of the Lassen Peak dome provide a unique opportunity to exposure-date young surfaces with cosmogenic ^{21}Ne. Even though measurement precision for ^{21}Ne concentrations and resulting ages on LGM deposits are still not as good as for ^{10}Be ages reported on contemporary moraines deposited in other sites in the Cascade~~s~~ Range and Sierra Nevada ~~Range~~, our ages broadly align with these other sites, suggesting we captured the general timing of moraine emplacements in the region, and opening the door for future work dating late Pleistocene moraines with ^{21}Ne.

2 Background and Setting

The landscape surrounding Lassen Volcanic National Park is dominated by ~~complex~~ volcanic eruptive sequences ranging in age from 3.5 Ma to present (Clynne and Muffler, 2010; Muffler and Clynne, 2015; Clynne and Muffler, 2017). The latest sequences of volcanic activity, which formed the LVC, began ~825 ka. Since then, there have been three eruptive episodes. The youngest of these episodes, referred to here as the Lassen domefield, began ~315 ka and is currently active. The latest activity occurred in 1914-1917 when a vent at the top of Lassen Peak erupted. The Lassen domefield is further subdivided by

both age and lithology (see Fig. 8 in Muffler and Clynne, 2015); we focus on the Eagle Peak sequence (~115 ka – present; Germa et al., 2019) during which Lassen Peak formed. The Eagle Peak sequence consists of~~describes~~ geologic units from eight distinct eruptions in the park, and one of the youngest and most prominent geologic units is the dacite of Lassen Peak (unit dl in Clynne and Muffler, 2010). Outcrops of the dacite of Lassen Peak in the park are generally restricted to areas near Lassen Peak, but boulders, blocks and debris of the dacite are incorporated into extensive~~pansive~~ surficial deposits, including the pyroclastic and debris flows associated with the eruption at Lassen Peak in 1915, late Pleistocene glacial tills draped over the landscape near Lassen Peak, and glacial outwash in nearby valleys far down (at least 30 km) from Lassen Peak. Radiometric Ar/Ar dating of the unit indicates that the dacite of Lassen Peak was erupted at 28.3 ± 2.7 ka (Turrin et al., 1998). Several lines of evidence show that the dome was glaciated during the LGM as well (Turrin et al., 1998; Clynne and Muffler, 2010; Fig. 2). Such lines of evidence include abundant moraines and other glacial deposits incorporating sediments and blocks derived from the dacite of Lassen Peak, and evidence that the mantle of hot, prismatically jointed talus blocks that formed the eruptive carapace on Lassen Peak was almost completely stripped by glaciation (Clynne and Muffler, 2010).

The dacite of Lassen Peak is a lithologically homogeneous dome and lithic pyroclastic-flow deposit. The lava dome is a porphyritic dacite with 30% phenocrysts of plagioclase, hornblende, quartz and biotite in a glassy to aphanitic, weakly magnetic groundmass. The dacite contains 4% quartz with grain sizes ranging 1-2 mm (rarely to 5 mm). ~~The lava dome is a porphyritic dacite with 30% phenocrysts of quartz (up to 10%), plagioclase, hornblende, and biotite in a glassy to aphanitic, weakly magnetic groundmass.~~ The rock also contains small amounts of clinopyroxene and olivine derived from disaggregated mafic inclusions. It is the combination of abundant quartz and clinopyroxene that makes the dacite of Lassen Peak distinctive among other dacites in the Lassen domefield (Clynne and Muffler, 2010).

Zircon dating and trace-element analysis suggests that the quartz must have been stored at a sub-liquidus temperature in a 'crystal mush' phase between ~190 ka and the eruption of Lassen Peak at 28.3 ± 2.7 ka ~~(Klemetti and Clynne, 2014),~~ and that the periodic infusion of mafic magma caused the dome eruption and other recent volcanic activity (Klemetti and Clynne, 2014). Given the relatively young age of the dacite of Lassen Peak, the volcanic and glacial setting of the LVC, and the abundance~~t availability~~ of quartz phenocrysts, we hypothesized that the dacite of Lassen Peak might be a good target for surface-exposure dating of late Pleistocene surficial deposits using cosmogenic ^{21}Ne.

Prior to, and following the LVC dome eruption at ~28 ka, it is likely that large ice caps smothered the ~~surrounding~~ landscape in and around Lassen Volcanic National Park (Fig. 2; Turrin et al., 1998) as global climate transitioned to glacial periods during, for example, Marine Isotope Stage 6 and 2 (MIS 6; 191–130 ka; MIS 2; 29–11 ka; Lisiecki and Raymo, 2005). Whereas there are no absolute ages on glacial deposits in and around the LVC, Clynne and Muffler (2010) summarized previous mapping efforts and subdivide glacial deposits into 'older' and 'younger' tills, where the older tills correlate to the regionally identified Tahoe Glaciation (likely MIS 6; Laabs et al., 2020) and the younger tills correlate to the Tioga

Glaciation (constrained to MIS 2), known locally as the Anklin Meadows glaciation (Turrin et al., 1998). Moraines in several drainages around Lassen Peak have been identified and mapped (Turrin et al., 1998; Christiansen et al., 2002), and Anklin Meadows moraines have been subdivided largely by their elevation, stratigraphic position, soil development, and the presence/absence of known age lithologies comprising the sediments and blocks embedded in the moraines. The only current absolute dates that help constrain the ages of moraines in the LVC containing dacite of Lassen Peak debris come from indirect radiocarbon constraints that bracket the radiometric $^{40}Ar/^{39}Ar$ date of the dacite of Lassen Peak from Turrin et al. (1998); there currently are no direct dates on moraines in the LVC.

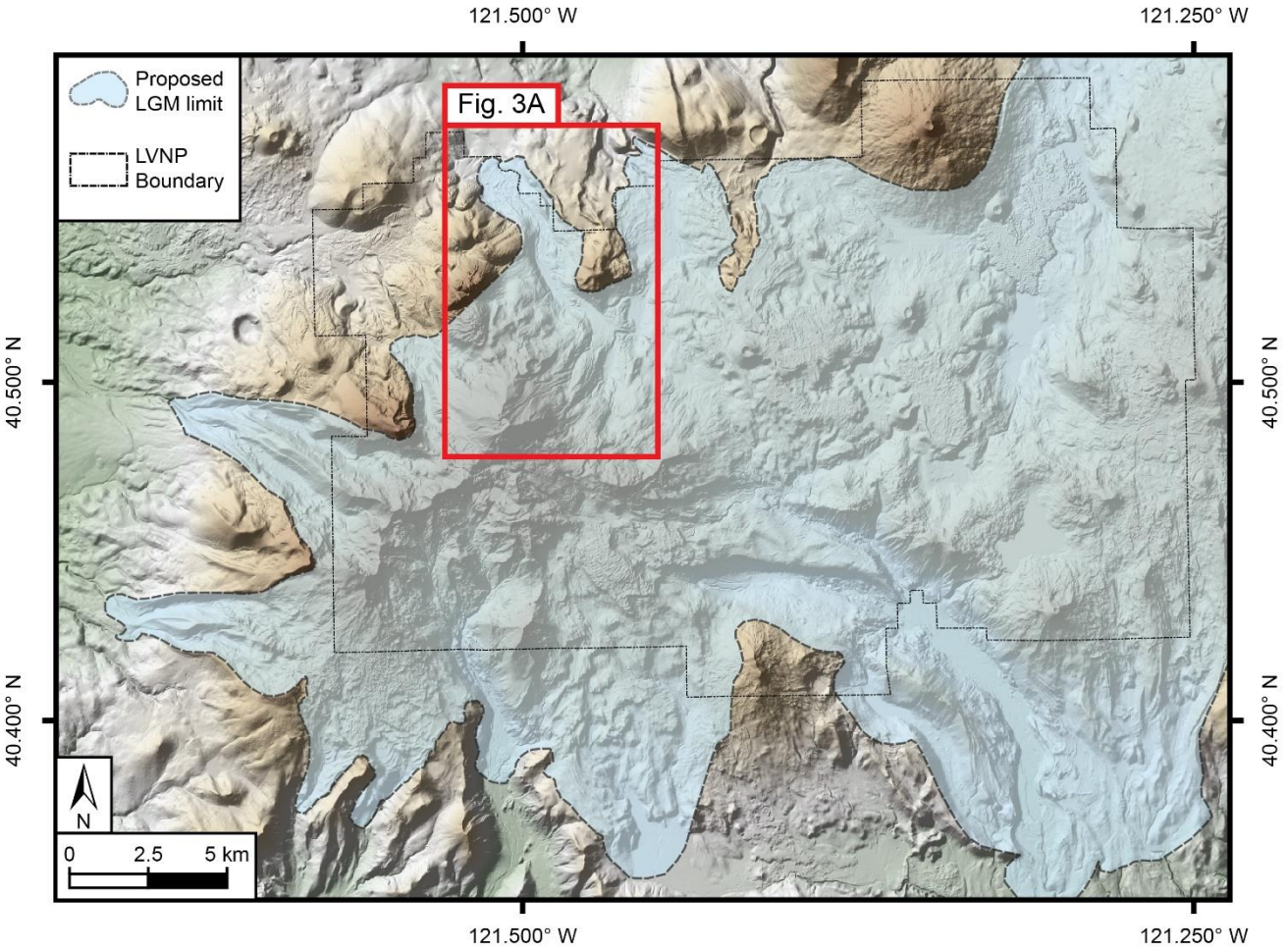

Figure 2. Map of Lassen Volcanic National Park and vicinity. Dot-dot-dash lines are park boundary, light blue transparent shade is the proposed limit of LGM glaciation in the region (adapted from Clynne and Muffler, 2010). Basemap and hillshade are from the 1/3 arc-second digital elevation model made available through the USGS National Map 3D Elevation Program (https://www.usgs.gov/programs/national-geospatial-program/national-map date of last access; Feb 1, 2024).

Turrin et al. (1998, and later updated in Clynne and Muffler, 2010), described several sets of Anklin Meadows moraine units in Lost Creek drainage (Fig. 3); we targeted moraines mapped from the two oldest units, Anklin Meadows A1 and A2. The

oldest and lowest-elevation moraines (Anklin Meadows A1) are found around 1600-1700 m asl in Lost Creek drainage. Anklin Meadows A2 moraines were deposited around 1950 m asl. Below, we describe two moraines mapped within the A1 unit (Lost Creek Moraine 1 and Lost Creek Moraine 2; Fig. 3A and 3B), and one moraine mapped within the A2 unit (Lost Creek Moraine 3; Fig. 3A and 3C). All moraines in the Lost Creek drainage contain abundant boulders up to 4 m in diameter of dacite of Lassen Peak transported by ice that flowed from Lassen Peak down-valley. In the Lost Creek drainage, large avalanche and debris flow deposits from the 1915 eruption (which include entrained massive blocks sourced from the dacite of Lassen Peak) follow the center of the drainage, but these deposits did not override the moraines that we targeted for exposure dating (Christiansen et al., 2002).

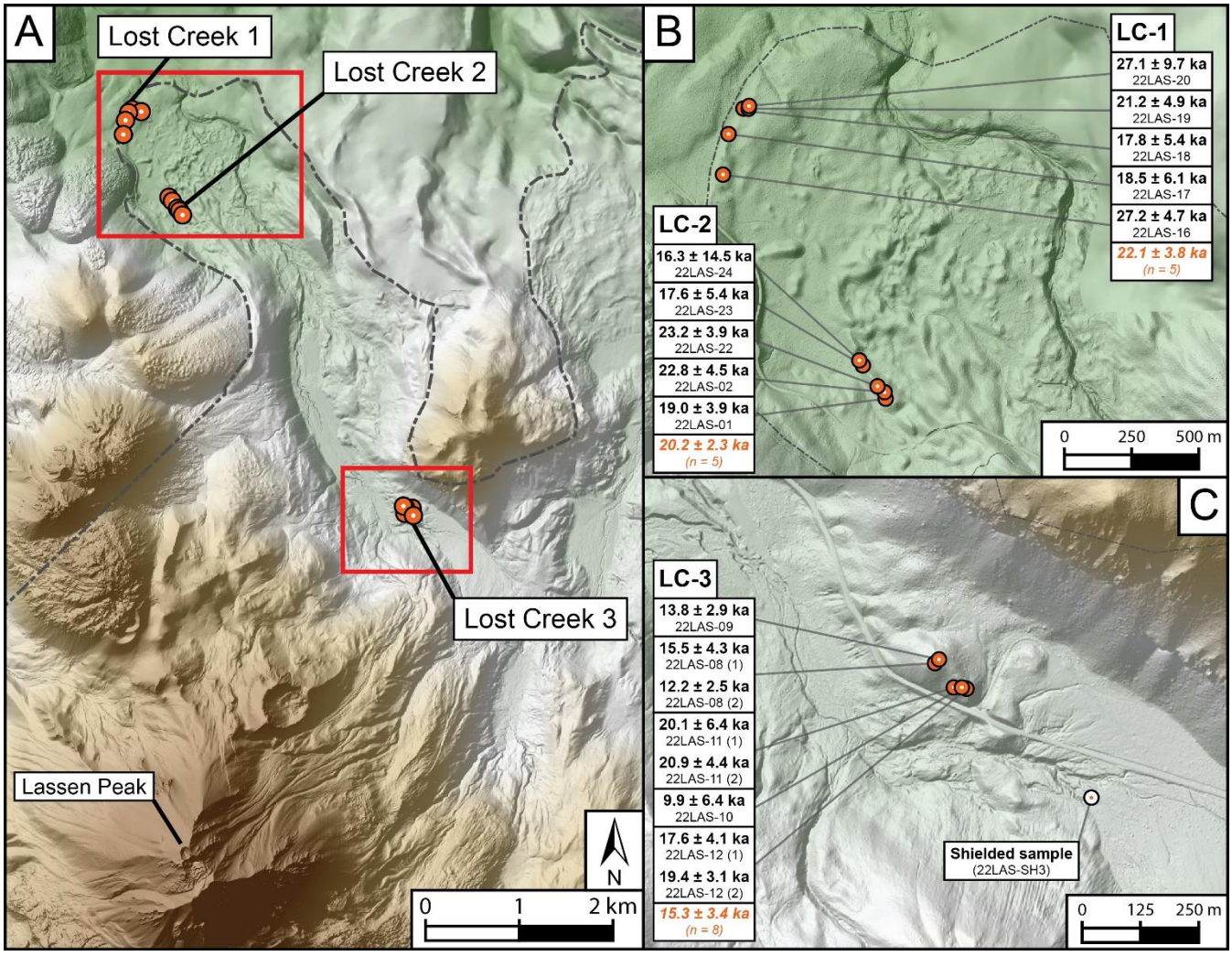

Figure 3. Lost Creek drainage north of Lassen Peak. A). A: ~~Complete~~ Lost Creek drainage with sample locations highlighted for each moraine (Lost Creek 1, 2 and 3). B: Zoom in on Lost Creek 1 and Lost Creek 2 (A1) moraines. Samples listed with calculated ages and internal uncertainties. Average moraine ages in orange text. C: Zoom in on Lost Creek moraine 3 (A2) up-valley from

Lost Creek moraines 1 and 2. Individual ages and moraine ages reported in the same way as panel B. Note the multiple aliquots measured for samples 22LAS-08, 22LAS-11 and 22LAS-12. Location of the large block entrained in the 1915 avalanche and debris flow used to procure a shielded sample noted in panel C. Basemap and hillshade are sourced from post-processed, Lidar-based digital elevation model products available through the USGS National Map 3D Elevation Program (https://www.usgs.gov/programs/national-geospatial-program/national-map date of last access; Feb 1, 2024).

3 Materials and methods

3.1 Sample collection and processing

We collected surface samples for cosmogenic ^{21}Ne exposure dating from 15 boulders sourced from the lithologically homogeneous dacite of Lassen Peak on the crests of three distinct moraines in the Lost Creek drainage in summer 2022. We sampled five boulders on each moraine. We targeted large (1–2 m tall; Fig. 4; see ~~www.ice-d.org~~ https://www.ice-d.org/alpine/publication/1200/ for all field sample photos) tabular boulders with low-sloping top surfaces to limit the impact of surface erosion. In addition to reduced snow cover from wind-sweeping, the tops of large boulders are also better shielded from forest ~~–~~fire activity, which has the potential to heat surfaces to the point where ^{21}Ne can diffuse out of quartz (Shuster and Farley, 2005). We extracted approximately 1 kg of sample from the surface of each boulder using a carbide tipped power drill, steel wedges, and a hammer. We recorded longitude and latitude using a handheld GPS and calculated topographic- and self-shielding corrections using in-field measurements with a smartphone app clinometer and the shielding correction calculator from the online exposure age calculator website (https://hess.ess.washington.edu/).

Table 1. Field observations and analytical measurements for sampled boulders

Sample name	Latitude (DD)	Longitude (DD)	Elevation (m a.s.l)	Sample thickness (cm)	Shielding Correction	quartz weight (g)	Ne-21 TOT (atoms 10^6)	Ne-21 excess (atoms 10^6)	Ne-21 excess (%)	[Ne-21 excess] (atoms/g 10^6)	Ne-21 exposure age (ka)
Lost Creek Moraine 1											
22LAS-16	40.56015	-121.51479	1718	1.0	1.000000	0.2952	1.14 ± 0.08	0.517 ± 0.09	45.4	1.75 ± 0.306	27.2 ± 4.7
22LAS-17	40.56150	-121.51450	1713	1.0	1.000000	0.4647	2.53 ± 0.15	0.552 ± 0.182	21.9	1.187 ± 0.392	18.5 ± 6.1
22LAS-18	40.56234	-121.51382	1711	2.0	1.000000	0.3992	1.86 ± 0.12	0.45 ± 0.137	24.2	1.127 ± 0.344	17.8 ± 5.4
22LAS-19	40.56235	-121.51363	1713	1.5	1.000000	0.4933	2.27 ± 0.13	0.669 ± 0.155	29.4	1.356 ± 0.314	21.2 ± 4.9
22LAS-20	40.56243	-121.51358	1712	2.0	1.000000	0.2757	2.45 ± 0.15	0.483 ± 0.173	19.7	1.751 ± 0.628	27.1 ± 9.7
Lost Creek Moraine 2											
22LAS-01	40.55251	-121.50780	1767	2.5	1.000000	0.4990	2.15 ± 0.11	0.615 ± 0.126	28.5	1.232 ± 0.252	19.0 ± 3.9
22LAS-02	40.55272	-121.50785	1768	2.0	1.000000	0.4131	1.68 ± 0.11	0.627 ± 0.122	37.4	1.517 ± 0.296	22.8 ± 4.5

22LAS-22	40.55292	-121.50816	1764	2.0	1.000000	0.4417	1.33 ± 0.09	0.613 ± 0.102	46.2	1.387 ± 0.231	23.2 ± 3.9
22LAS-23	40.55364	-121.50880	1754	2.0	1.000000	0.2638	1.16 ± 0.08	0.298 ± 0.09	25.6	1.129 ± 0.343	17.6 ± 5.4
22LAS-24	40.55379	-121.50892	1753	2.0	1.000000	0.4711	6.9 ± 0.34	0.487 ± 0.433	7.1	1.033 ± 0.919	16.3 ± 14.5
Lost Creek Moraine 3											
22LAS-08 (a)	40.52369	-121.48016	1950	3.0	0.992568	0.4085	1.61 ± 0.11	0.457 ± 0.126	28.4	1.12 ± 0.308	15.5 ± 4.3
22LAS-08 (b)	-	-	-	-	-	0.4240	1.33 ± 0.07	0.378 ± 0.077	28.4	0.892 ± 0.182	12.2 ± 2.5
22LAS-09	40.52376	-121.48004	1950	1.0	0.992568	0.5300	1.73 ± 0.1	0.535 ± 0.112	30.9	1.009 ± 0.212	13.8 ± 2.9
22LAS-10	40.52318	-121.47945	1941	1.5	0.992568	0.4875	3.16 ± 0.19	0.359 ± 0.232	11.4	0.736 ± 0.476	9.9 ± 6.4
22LAS-11 (a)	40.52319	-121.47965	1939	1.5	0.992568	0.4462	2.41 ± 0.15	0.524 ± 0.177	21.8	1.174 ± 0.396	20.1 ± 6.4
22LAS-11 (b)	-	-	-	-	-	0.4282	3.7 ± 0.11	0.668 ± 0.14	18.1	1.561 ± 0.326	20.9 ± 4.4
22LAS-12 (a)	40.52316	-121.47933	1942	2.0	0.992568	0.3804	1.59 ± 0.1	0.49 ± 0.113	30.8	1.287 ± 0.298	17.6 ± 4.1
22LAS-12 (b)	-	-	-	-	-	0.4063	1.81 ± 0.08	0.582 ± 0.093	32.2	1.433 ± 0.228	19.4 ± 3.1
dacite of Lassen Peak Shielded Sample											
22LAS-SH3	-	-	-	-	-	0.4567	4.02 ± 0.21	not detected	not detected	not detected	-

Notes: all samples are sourced from the dacite of Lassen Peak, thus sample density assumed to be 2.~~86~~0 g/cm^3 for all samples. Three samples (22LAS-08, 22LAS-11, and 22LAS-12) that have two aliquots measured on each are labeled with (a) and (b) to distinguish aliquots. All additional neon measurements and analyses are reported in the supplementary table S1. All measurement uncertainties are reported as 1-sigma.

We also procured a sample from the underside of a large (>5m tall) block of dacite of Lassen Peak entrained in the 1915 avalanche and debris flow in the Lost Creek drainage, for the purpose of constraining the nucleogenic component of ^{21}Ne-excess (see below). The upward-facing surface of the large tabular block displayed evidence of glacial sculpting (Fig. 4; e.g., striations), so we interpret that the top of the block was exposed after deglaciation, plucked, and entrained in the avalanche and debris flow during the 1915 eruption and deposited glacially sculpted side up. Thus, it is likely that the underside of the block where we sampled was completely shielded from the cosmic-ray flux following formation and through the eruption, plucking, and deposition process.

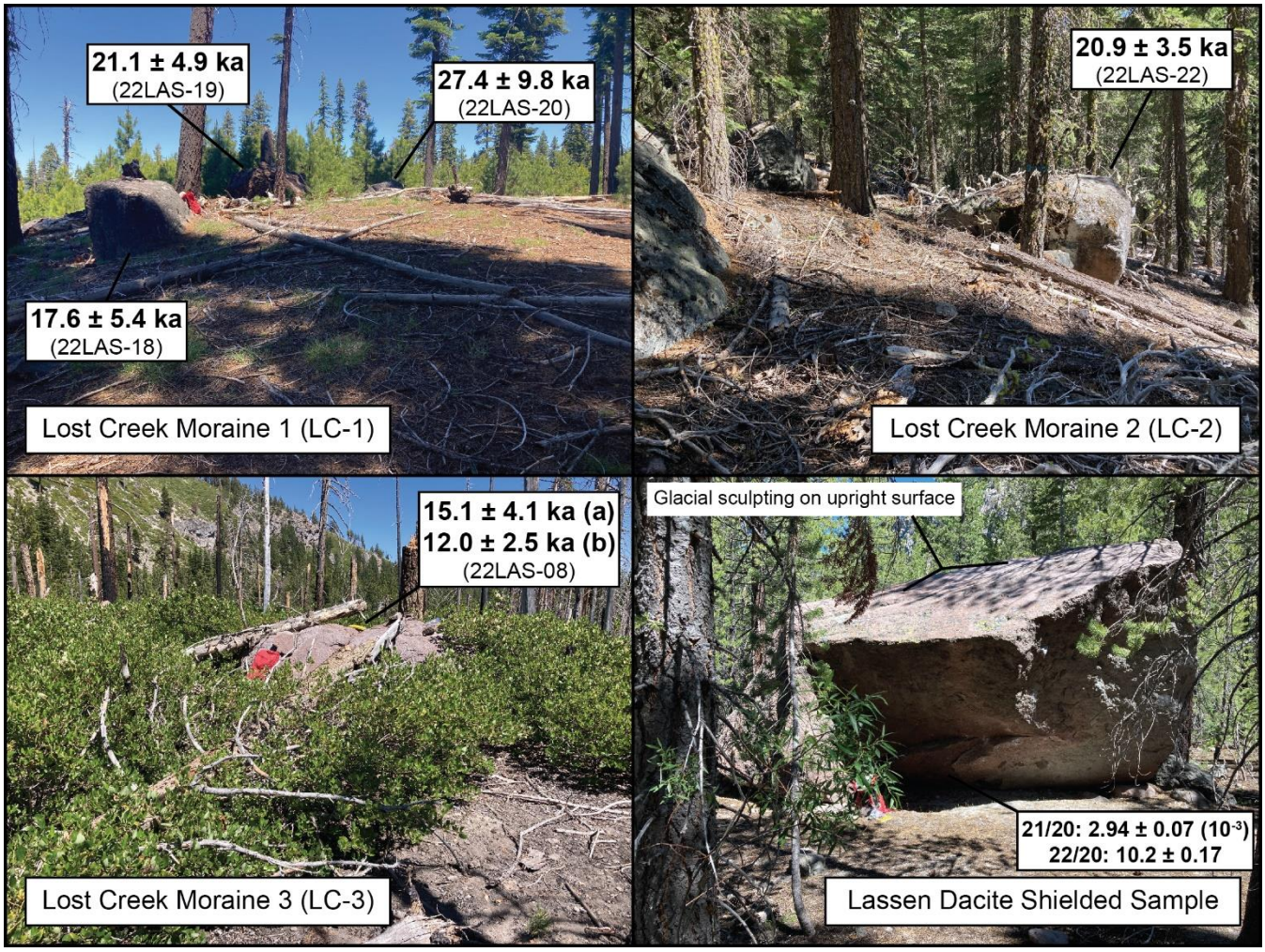

Figure 4. Example field sample photos, one per moraine. Clockwise from top left: Three samples clustered nearby on the outermost LGM moraine, Lost Creek 1, one boulder embedded in the Lost Creek 2 moraine, the large block sourced from the dacite of Lassen Peak that was entrained in the 1915 avalanche and debris flow with approximate location of underside sample collection noted, and one boulder with two aliquots measured from the collected surface sample on the Lost Creek 3 moraine. Moraine boulders are shown with calculated ages and internal uncertainties (Photo credits: JP Tulenko).

We prepared all samples, including the ‘shielded’ sample, at the Berkeley Geochronology Center (BGC) rock preparation lab and then the University at Buffalo (UB) cosmogenic isotope lab. We crushed sample fractions of approximately 150 g from each total sample (sample thicknesses reported here are the thicknesses of the sample fractions that were crushed) using a mortar and pestle and sieved to 300-600 microns (BGC). We rinsed this target fraction and separated magnetic minerals using a Frantz magnetic separator, leaving quartz and plagioclase (BGC). To isolate quartz from plagioclase, we used the froth flotation method (see Corbett et al., 2016) before etching the quartz-rich fractions in low-concentration HF (~2-3%) at room temperature for several weeks to remove any remaining plagioclase and the outside of the quartz grains that may have

been enriched in nucleogenic ^{21}Ne derived from alpha implantation through U and ~~/~~Th decay in adjacent minerals or glass (UB; see Niedermann, 2002 for more details).

3.2 Analytical measurements

We measured all three neon isotopes (^{20}Ne, ^{21}Ne, ^{22}Ne) in purified quartz on the "Ohio" noble~~-~~gas mass spectrometer (NGMS) system at the Berkeley Geochronology Center (see supplement for complete data report). The NGMS system consists of a MAP-215 sector~~-~~field mass spectrometer with modernized ion-counting electronics coupled to a fully automated gas extraction system. We encapsulated ~0.4 g aliquots of quartz in tantalum packets and heated them under vacuum using a 150W, 810 nm diode laser, in two heating steps at 950° C and 1200° C. Reactive gases were removed by exposure to a SAES Getter, remaining noble gases were frozen to an activated charcoal trap at 33 K, non-adsorbed gases (presumably mostly He) were pumped away, and Ne was released to the mass spectrometer at 75 K.

All three isotopes of neon were measured by ion-counting, with corrections for CO_2^{++} on mass 22 and $^{40}Ar^{++}$ on mass 20 made using an ^{39}Ar spike (Balco and Shuster, 2009). Absolute Ne concentrations are determined by peak height comparison with an air standard measured several times daily. Mass discrimination corrections are also based on the air standard. Reported uncertainties include counting uncertainties on all masses (including those used for correction of isobars), correction for an extraction line "cold" blank measured without any introduction of sample, and the reproducibility of the air standard. "Hot" blanks that included heating of empty metal packets released small amounts of neon with atmospheric isotope composition, so this contribution is accounted for in the calculation of excess ^{21}Ne, and a separate hot blank correction was not made. The amount and isotopic composition of neon released in all 1200° C steps was indistinguishable from that released in the hot blanks, so we conclude that the samples were fully degassed at 950° C, and report only the results of the first heating steps. Three aliquots of the CRONUS-A standard analyzed during the period of this study yielded excess ^{21}Ne concentrations of 336.1 ± 8.1 x 10^6 ~~M~~atoms/g. This is slightly more than the nominal value for this standard of 320 x 10^6 ~~M~~atoms/g (Vermeesch et al., 2015). Although in Table 1 we report data as measured, excess ^{21}Ne concentrations are renormalized to the nominal value of 320 x 10^6 atoms/g when calculating exposure ages, as described below.

3.3 Cosmogenic ^{21}Ne measurements and age calculations

From the measured neon isotope results we then calculated excess ^{21}Ne as follows:

$$^{21}Ne_{xs} = {}^{21}Ne_{tot} - \left(Ra_{21/20} * {}^{20}Ne_{tot}\right)$$

w~~W~~here $^{21}Ne_{xs}$ is excess ^{21}Ne relative to atmosphere, $Ra_{21/20}$ is the atmospheric ^{21}Ne/^{20}Ne ratio (0.002959; Dunai, 2010), $^{21}Ne_{tot}$ is total measured ^{21}Ne, and $^{20}Ne_{tot}$ is total measured ^{20}Ne. As shown below in the results (and in the supplementary table), excess ^{21}Ne in the shielded sample was indistinguishable from zero. Thus, as all samples are from the lithologically homogeneous dacite of Lassen Peak, ~~, so~~ we take excess ^{21}Ne to be equivalent to cosmogenic ^{21}Ne in all samples. We then computed cosmogenic ^{21}Ne exposure ages using version 3 of the online exposure age calculator described by Balco et al.

(2008) and subsequently updated, with the LSDn scaling method (Lifton et al., 2014, 2016) and production rate calibration data from the SPICE project in Arizona, USA (Fenton et al., 2019; full dataset available on ICE-D at https://www.ice-d.org/production%20rate%20calibration%20data/cal_data_set/13). As mentioned above, exposure-age calculations in the online calculator include normalization to the nominal value of 320 x 10^6 Matoms/g for CRONUS-A. Further, we assume negligible post-depositional boulder surface erosion and snow cover as a common community practice, which means that all ages presented here are minimum exposure ages.

4 Results

As hypothesized, quartz in the dacite of Lassen Peak has an undetectable amount of nucleogenic ^{21}Ne and unusually low concentrations of atmospheric neon. First, ^{21}Ne/^{20}Ne and ^{22}Ne/^{20}Ne ratios in the shielded sample are 0.00294 ± 0.0007 and 0.1025 ± 0.0017, respectively, which are indistinguishable from atmosphere (Figure 5). This implies that nucleogenic ^{21}Ne in quartz in this lithology is negligible and, in addition, provides no evidence for the presence of any trapped magmatic neon. Thus, as noted above, we calculated excess ^{21}Ne to be equivalent to cosmogenic ^{21}Ne. Second, concentrations of atmospheric neon in quartz in this lithology, expressed as ^{21}Ne, are 4.4 ± 3.0 x 10^6 Matoms/g ^{21}Ne (mean and 1 standard deviation of all samples), which, although still greater than concentrations of cosmogenic ^{21}Ne in the 0.75-1.5 x 10^6 Matoms/g range, are substantially lower than in most other measured rocks to date.

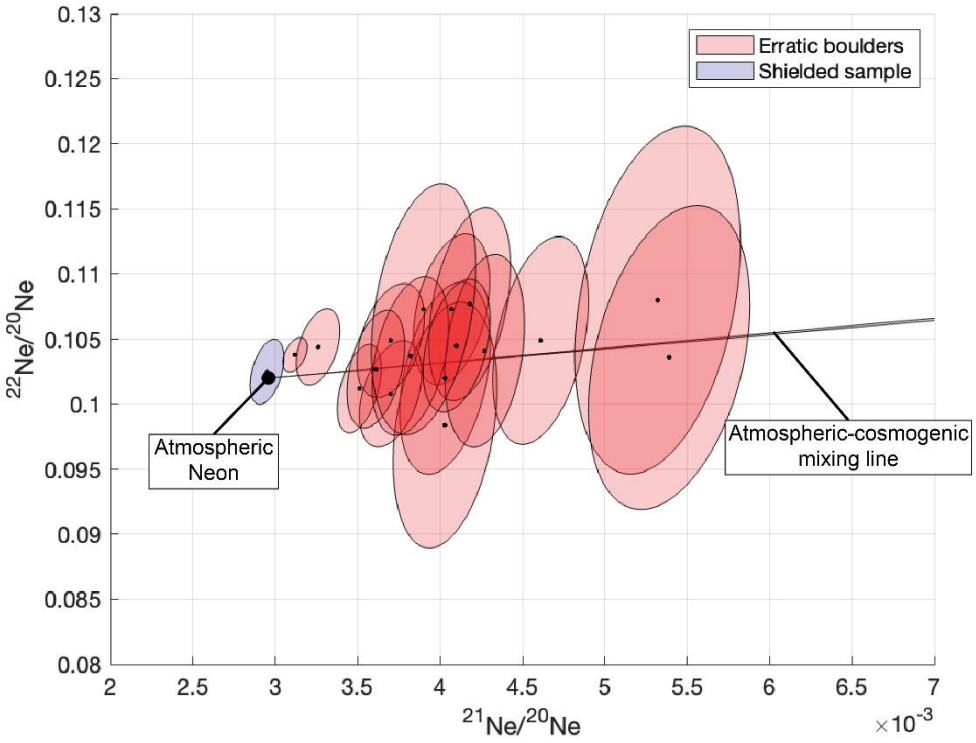

Figure 5. Neon three-isotope plot for all 950° C heating steps. The black dot is the composition of atmospheric neon, and the black line is the atmospheric-cosmogenic mixing line (Niedermann, 2002). The ellipses are 68% confidence regions. The isotope composition of neon in the shielded sample is indistinguishable from atmosphere, indicating a negligible concentration of nucleogenic or magmatic neon. All other data lie on or near the atmospheric-cosmogenic mixing line within uncertainty.

Cosmogenic ^{21}Ne concentrations in moraine boulder samples in the Lost Creek drainage range from ~0.736 – 1.751 x 10^6 ~~M~~atoms/g and account for ~27 ± 9% of the total measured ^{21}Ne in each sample (Table 1), with the remaining fraction being attributable to atmospheric ^{21}Ne. Calculated ^{21}Ne exposure ages for all samples range from 27.1 ± 9.7 ka to 9.9 ± 6.4 ka (Table 1; Figure 6). Ages from each moraine comprise single populations. On the outermost terminal LGM moraine (LC-1), 5 ages from 5 boulders average to 22.1 ± 3.8 ka (moraine ages reported here and throughout are the arithmetic mean and one standard deviation, without propagating an additional production rate uncertainty). A few hundred meters up-valley, 5 ages from 5 boulders on the next dated moraine (LC-2) average to 20.2 ± 2.3 ka. ~~Finally, 4 km up-valley from LC-1 and LC-2, 8 ages from 5 boulders (with replicate measurements on 22LAS-08, 22LAS-11, and 22LAS-12) from the innermost recessional moraine dated in the Lost Creek Drainage (LC-3) average 15.3 ± 3.4 ka.~~ Finally, to determine the average age of the LC-3 moraine 4 km up-valley from LC-1 and LC-2, 8 ages from 5 boulders (with replicate measurements on 22LAS-08, 22LAS-11, and 22LAS-12) from the innermost recessional moraine dated in the Lost Creek Drainage (LC-3) were calculated. First, we calculated the average age and root mean square error – propagating each individual measurement uncertainty and the 1 standard deviation of the two ages – for each individual boulder that had replicate measurements (3

boulders, 22LAS-08 at 13.9 ± 5.2 ka, 22LAS-11 at 20.5 ± 7.7 ka, and 22LAS-12 at 18.5 ± 5.2 ka). Then, we calculated a simple arithmetic mean moraine age for LC-3 using those average boulder ages along with the calculated ages of the other two boulders with just one measurement on them (22LAS-09, 22LAS-10). Thus, the average age of the LC-3 moraine using approach is 15.3 ± 3.8. We suggest this approach because the difference in ages on the replicate boulders (e.g., LAS22-08 has 15.5 ka and 12.2 ka ages that are ~3.3 kyr offset) is likely more impacted by measurement uncertainty and reproducibility during the mass spectrometry measurement process than from any geologic uncertainty. The quartz measured in each replicate comes from the same processed material so geologic uncertainties (e.g., sampling from different locations on the boulder surface, grain size, etc.) would not impact the measurements. ~~Thus,~~We find that ages for the three moraines are in stratigraphic order.

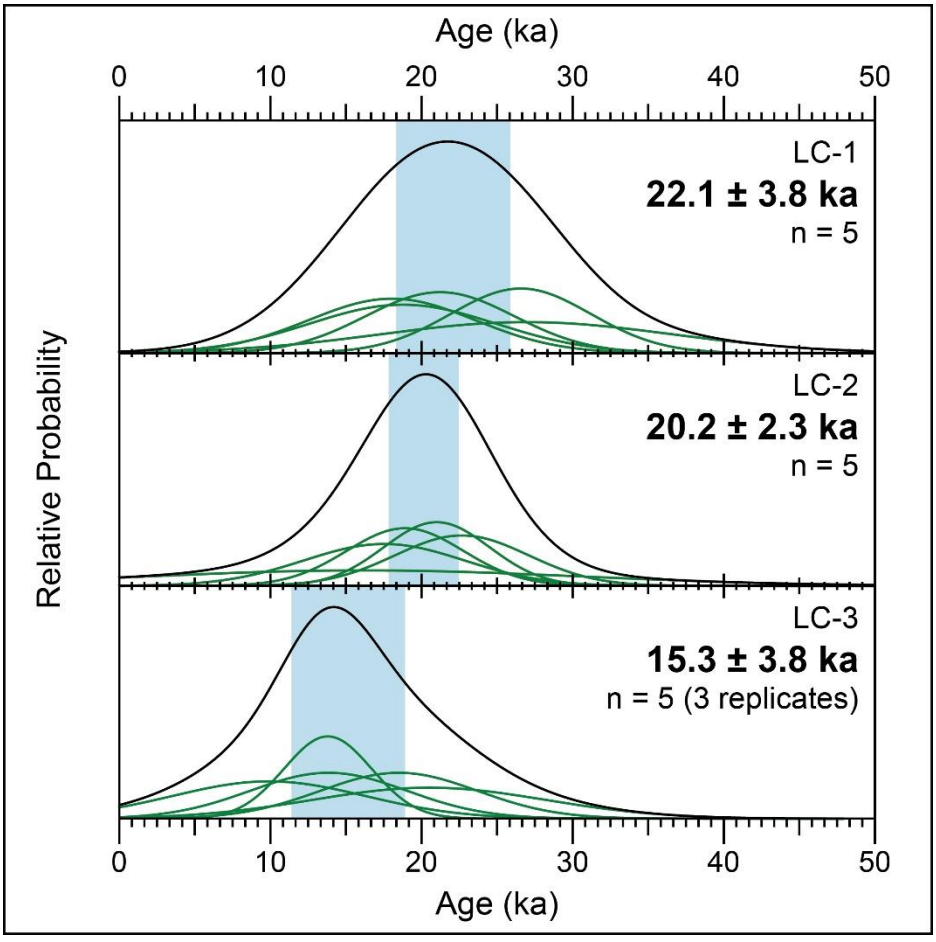

Figure 6. Individual probability density functions (pdfs) for each sample (green) and summed pdfs for each moraine age (black). Individual pdfs are based on the calculated age and internal uncertainty for each sample. Blue bars indicate the mean and 1 standard deviation of the ages on each moraine.

5 Discussion

We now assess 1) the efficacy of the dating method itself for late Pleistocene deposits and 2) the power of resolving local glacial and climate histories based on the results.

5.1 Cosmogenic ^{21}Ne exposure dating of the dacite of Lassen Peak

Our initial hypothesis, that due to the relatively young age and rapid rate of cooling of the dacite of Lassen Peak the nucleogenic and atmospheric ^{21}Ne concentrations in this lithology are relatively low, is supported by the measurements. This demonstrates that the dacite of Lassen Peak is a favorable target for ^{21}Ne exposure dating.

Although this is not the first study to take advantage of the low ^{21}Ne background in young quartz-bearing volcanic rocks (for example, see work on depth-profile dating of alluvial fans composed of the Bandelier Tuff in New Mexico, USA by Phillips et al., 1998), to the best of our knowledge, the moraines described here are the youngest landforms successfully exposure-dated using ^{21}Ne to date in any published study. However, although the dacite of Lassen Peak is among the best-case scenarios for dating recently exposed surfaces with cosmogenic ^{21}Ne, we still find that a majority of the total ^{21}Ne inventory is non-cosmogenic (Table 1), which limits the precision of the dating method. This is especially true in comparison with ^{10}Be measurements that produce uncertainties up to an order of magnitude lower than those reported here, 2-3% versus ~20-30%. However, considering the total cost of analyses and preparation time for ^{10}Be measurements – which can be up to an order of magnitude more expensive – cosmogenic ^{21}Ne, in unique situations like these, might be a suitable avenue to efficiently test broad generalized hypotheses and provide a proof-of-concept for further, more detailed investigation with higher-precision techniques. Moreover, measurement uncertainties can be slightly reduced, for example, by measuring multiple aliquots on individual samples and taking the weighted mean (similar to what was done for samples 22LAS-08, 11 and 12), which could be a worthwhile endeavor in future work if time and resources are available. Topics of study could include further glacial history reconstructions as presented here, long-term fault slip rates by measuring offset surficial features (e.g., Rood et al., 2011), and volcanic histories (e.g., Valentine et al., 2019) in such places where young, quartz-bearing volcanic rocks exist.

5.2 Deglacial history of the LVC in the context of the broader Cascade~~s~~ Range and Sierra Nevada ~~Range~~ region

Moraine ages in Lost Creek indicate that the LGM may have culminated in Lassen Volcanic National Park ca. 22 ka (LC-1), with ice remaining near the maximum extent for another ~2 kyr, to emplace a recessional moraine (LC-2) ca. 20 ka. There are additional moraines and hummocky terrain just inboard of the LC-2 moraine that have not yet been sampled, but an additional dated recessional moraine (LC-3) ~4 km up-valley indicates ~4 km of modest recession, then deposition of a moraine at ca. 15 ka.

We next compare our record of deglaciation in LVNP with a subset of all other sites (n = 13) around the Cascade~~s~~ Range and Sierra Nevada ~~Range~~, summarized in Figure 7. All data extracted for this comparison come from the ICE-D database (www.ice-d.org; last access: 09/01/2023; citations to the original data generators noted in each figure panel). ICE-D is capable of dynamically re-calculating cosmogenic nuclide exposure ages using internally consistent scaling schemes and the default production rate calibration from version 3 of the online exposure age calculator (https://hess.ess.washington.edu/). All ages extracted from this study were automatically re-calculated using the LSDn scaling scheme (Lifton et al., 2014) and default production rate from the online exposure age calculator (Borchers et al., 2016) to provide a consistent comparison between our samples and those measured in previous studies. Sites were identified specifically as moraines in the region with a minimum of four ages per moraine to increase the likelihood that ages compared reflect a true glacier termination and not other processes (e.g., boulder exhumation/moraine degradation). For each moraine, we systematically identified extreme

values/outliers by calculating the χ^2 statistic assuming a normal distribution. If the calculated p value – based on the χ^2 statistic and degrees of freedom per moraine – was below 0.1, we systematically pruned the individual sample with the most extreme individual χ^2 value until the dataset satisfied the criteria for a normal distribution. Then we simply calculated the mean and standard deviation to estimate the moraine age and uncertainty.

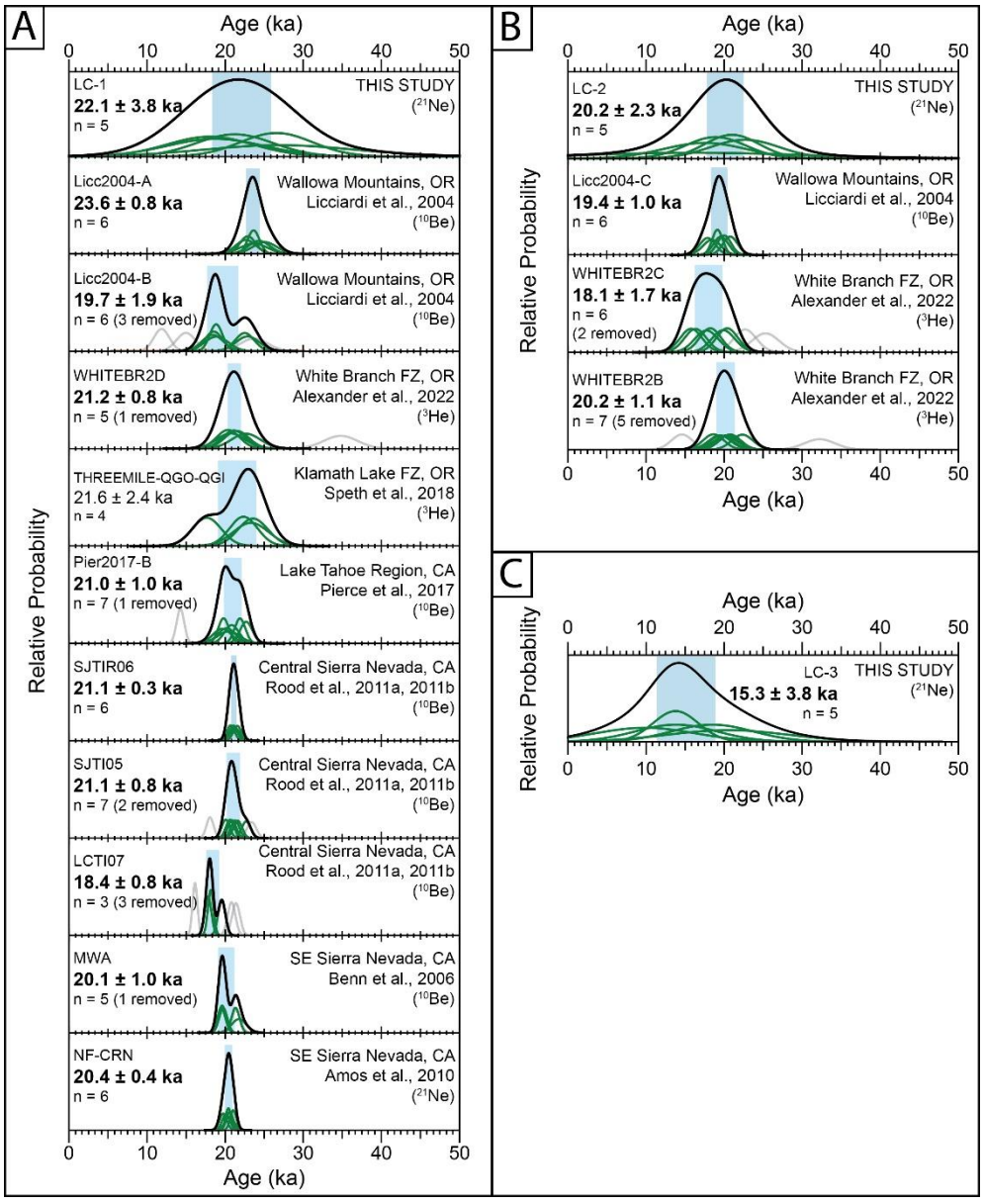

Figure 7. Individual and summed pdfs for moraines dated across the Cascades Range and Sierra Nevada Range. A) Terminal LGM moraine ages from the region listed from nNorth to sSouth (except for the terminal moraine from this study, LC-1, which is listed at the top), B) earliest recessional moraine ages in the region listed Nnorth to Ssouth, and C) the youngest recessional moraine dated in the LVC (LC-3). For each summed pdf, site (moraine) names from ICE-D, average ages, sample counts (excluding identified outliers noted in parentheses) and citations are reported. Individual ages included in the average age calculation are based on sample ages and internal uncertainties (like Fig. 6) and are plotted in green. Samples that were identified and excluded as outliers using an outlier rejection scheme are plotted in light grey. The solid black line is the summed pdf after outlier removal. The blue box in each plot is the mean and 1 standard deviation of all samples for each moraine. Note that site locations here correspond to site locations and citations denoted in Figure 1.

Terminal LGM moraine ages across the region range from ~23 to 18 ka, conforming with our ^{21}Ne-based moraine ages, within error. Moreover, a handful of the other sites around the region contain dated recessional

moraines ranging ~20 to 19 ka that also conform well with our LC-2 moraine. Some previously dated moraines contain a few ages older than the rest of the population of samples (e.g., WHITEBR2D and WHITEBR2B), which may indicate some instances of nuclide inheritance, but we consider those instances to be minimal. Thus, it is possible that whatever regional climatic controls acted on alpine glacial patterns in other sites across the region were also acting on the glaciers in the LVC. However, additional late Pleistocene recessional moraines to compare with the inner recessional moraine dated in Lost Creek drainage (LC-3) are not currently observed in the region. It is unclear whether this dearth is due to climatic forcing inhibiting moraine deposition at other sites during this time, the lack of preservation of similar recessional moraines in other valleys, or a lack of surveying and sampling, all of which currently remain unresolved. It is notable, however, that in other parts of the western US, such as the central Colorado Rocky~~ies~~ Mountains (e.g., Schweinsberg et al., 2020) and the Pioneer Mountains in SW Montana (Schoenemann et al., 2023), there is evidence of moraine deposition ca. ~15-16 ka, coinciding with timing of LC-3 moraine deposition at our site. Whether this is a result of regional climate or local factors in the LVC, higher-precision measurements and further investigation at our study site are required to resolve these new questions.

6 Conclusions

We present 18 new cosmogenic ^{21}Ne exposure ages on three distinct, inset moraines in Lassen Volcanic National Park, NE California, that average 22.1 ± 3.8 ka (n = 5), 20.2 ± 2.3 ka (n = 5), and 15.3 ± 3.4 ka (n = 8) on each respective moraine. Although the precision of our ^{21}Ne exposure ages is approximately an order of magnitude lower than ages from other sites in the Cascade Range and Sierra Nevada~~region~~, individual moraine ages that we measured are distinguishable and in stratigraphic order. The moraine ages indicate that the LGM may have culminated in LVNP in-step with other glaciated valleys across the Cascade~~s~~ Range and Sierra Nevada ~~Range~~, with a notable exception for the youngest moraine, LC-3, that appears to be unique to the LVC when compared to other sites in the Cascade Range~~s~~ and Sierra Nevada ~~Range~~ region. The results from this study present an example of an efficient and cost-effective means of estimating moraine ages using ^{21}Ne in quartz that could be further applied in the LVC and in other - likely limited - glaciated regions where quartz-bearing late Pleistocene-age volcanic rocks are present. Going forward, this approach may be employed - when targeting glaciated, young volcanic lithologies - as an initial surveying step in the process of generating precise deglacial records useful for reconstructing glacial and climate processes.

Author contributions

JPT: Conceptualization, Formal Analysis, Investigation, Data Curation, Writing – Original Draft, Visualization, GB: Conceptualization, Investigation, Data Curation, Writing – Review and Editing, Visualization, Funding Acquisition, MAC: Conceptualization, Investigation, Writing – Review and Editing, LJPM: Conceptualization, Writing – Review and Editing.

Competing Interests

At least one of the (co-)authors is a member of the editorial board of Geochronology.

Acknowledgements

We would like to thank the National Park Service in LVNP for permitting us to sample boulders within park boundaries, and Marie Bergelin for assistance with neon analyses at BGC. JPT was supported by NSF Grant number 1948416. The Berkeley Geochronology Center is supported in part by the Ann and Gordon Getty Foundation. Any use of trade, firm, or product names is for descriptive purposes only and does not imply endorsement by the U.S. Government. The LLNL contribution to this work was carried out under Contract DE-AC52-07NA27344. This manuscript is LLNL-JRNL-865941. Finally, we would like to acknowledge that samples were collected in the Lost Creek drainage on ancestral lands of the Atsugewi, and we give thanks to the original caretakers of these lands.

References

Alexander, K. A., Amos, C. B., Balco, G., Amidon, W. H., Clark, D. H., Meigs, A. J., and Lesnau, R. K.: Implications of glacial deposit ages for the timing and rate of active crustal faulting in the central Cascade arc, Oregon, USA, Geosphere, 18, 1726–1751, https://doi.org/10.1130/GES02476.1, 2022.

Amos, C. B., Kelson, K. I., Rood, D. H., Simpson, D. T., and Rose, R. S.: Late Quaternary slip rate on the Kern Canyon fault at Soda Spring, Tulare County, California, Lithosphere, 2, 411–417, https://doi.org/10.1130/L100.1, 2010.

Balco, G.: Contributions and unrealized potential contributions of cosmogenic-nuclide exposure dating to glacier chronology, 1990–2010, Quaternary Science Reviews, 30, 3–27, https://doi.org/10.1016/j.quascirev.2010.11.003, 2011.

Balco, G. and Shuster, D. L.: Production rate of cosmogenic ^{21}Ne in quartz estimated from ^{10}Be, ^{26}Al, and ^{21}Ne concentrations in slowly eroding Antarctic bedrock surfaces, Earth and Planetary Science Letters, 281, 48–58, https://doi.org/10.1016/j.epsl.2009.02.006, 2009.

Balco, G., Stone, J. O., Lifton, N. A., and Dunai, T. J.: A complete and easily accessible means of calculating surface exposure ages or erosion rates from ^{10}Be and ^{26}Al measurements, Quaternary Ggeochronology, 3, 174–195, https://doi.org/10.1016/j.quageo.2007.12.001, 2008.

Balco, G., Blard, P.-H., Shuster, D. L., Stone, J. O., and Zimmermann, L.: Cosmogenic and nucleogenic ^{21}Ne in quartz in a 28-meter sandstone core from the McMurdo Dry Valleys, Antarctica, Quaternary Geochronology, 52, 63–76, https://doi.org/10.1016/j.quageo.2019.02.006, 2019.

Balter-Kennedy, A., Bromley, G., Balco, G., Thomas, H., and Jackson, M. S.: A 14.5-million-year record of East Antarctic Ice Sheet fluctuations from the central Transantarctic Mountains, constrained with cosmogenic ^{3}He, ^{10}Be, ^{21}Ne, and ^{26}Al, The Cryosphere, 14, 2647–2672, https://doi.org/10.5194/tc-14-2647-2020, 2020.

Benn, D. I., Owen, L. A., Finkel, R. C., and Clemmens, S.: Pleistocene lake outburst floods and fan formation along the eastern Sierra Nevada, California: implications for the interpretation of intermontane lacustrine records, Quaternary Science Reviews, 25, 2729–2748, https://doi.org/10.1016/j.quascirev.2006.02.018, 2006.

Borchers, B., Marrero, S., Balco, G., Caffee, M., Goehring, B., Lifton, N., Nishiizumi, K., Phillips, F., Schaefer, J., and Stone, J.: Geological calibration of spallation production rates in the CRONUS-Earth project, Quaternary Geochronology, 31, 188–198, 2016.

Chmeleff, J., von Blanckenburg, F., Kossert, K., and Jakob, D.: Determination of the 10Be half-life by multicollector ICP-MS and liquid scintillation counting, Nuclear Instruments and Methods in Physics Research Section B: Beam Interactions with Materials and Atoms, 268, 192–199, 2010.

Christiansen, R. L., Clynne, M. A., and Muffler, L. J. P.: Geologic map of the Lassen Peak, Chaos Crags, and Upper Hat Creek area, California, US Geological Survey, 2002.

Clark, P. U., Dyke, A. S., Shakun, J. D., Carlson, A. E., Clark, J., Wohlfarth, B., Mitrovica, J. X., Hostetler, S. W., and McCabe, A. M.: The last glacial maximum, Sscience, 325, 710–714, https://doi.org/10.1126/science.1172873, 2009.

Clark, P. U., Shakun, J. D., Baker, P. A., Bartlein, P. J., Brewer, S., Brook, E., Carlson, A. E., Cheng, H., Kaufman, D. S., and Liu, Z.: Global climate evolution during the last deglaciation, Proceedings of the National Academy of Sciences, 109, E1134–E1142, https://doi.org/10.1073/pnas.1116619109, 2012.

Clynne, M. A. and Muffler, L. J. P.: Geologic map of Lassen Volcanic National Park and vicinity, California, US Geological Survey Scientific Investigations Map 2899, scale 1:50,000., 2010.

Clynne, M.A., and Muffler, L.J.P.: Geologic field-trip guide to the Lassen segment of the Cascades Arc, northern California: U.S. Geological Survey Scientific Investigations Report 2017–5022–K2, 65 p., https://doi.org/10.3133/sir20175022K2, 2017.

Corbett, L. B., Bierman, P. R., and Rood, D. H.: An approach for optimizing in situ cosmogenic ^{10}Be sample preparation, Quaternary Geochronology, 33, 24–34, https://doi.org/10.1016/j.quageo.2016.02.001, 2016.

Dalton, A. S., et al.: An updated radiocarbon-based ice margin chronology for the last deglaciation of the North American Ice Sheet Complex, Quaternary Science Reviews, 234, 106223, https://doi.org/10.1016/j.quascirev.2020.106223, 2020.

Dunai, T. J., López, G. A. G., and Juez-Larré, J.: Oligocene–Miocene age of aridity in the Atacama Desert revealed by exposure dating of erosion-sensitive landforms, Geology, 33, 321–324, https://doi.org/10.1130/G21184.1, 2005.

Dunai, T. J.: Cosmogenic nuclides: principles, concepts and applications in the earth surface sciences, Cambridge University Press, 2010.

Fenton, C. R., Niedermann, S., Dunai, T., and Binnie, S. A.: The SPICE project: Production rates of cosmogenic ^{21}Ne, ^{10}Be, and ^{14}C in quartz from the 72 ka SP basalt flow, Arizona, USA~~u~~, Quaternary Geochronology, 54, 101019, https://doi.org/10.1016/j.quageo.2019.101019, 2019.

Germa, A., Perry, C., Quidelleur, X., Calvert, A., Clynne, M., Connor, C. B., Connor, L. J., Malservisi, R., and Charbonnier, S.: Temporal relationship between the Lassen volcanic center and mafic regional volcanism, Bulletin of Volcanology, 81, 1–17, https://doi.org/10.1007/s00445-019-1296-7, 2019.

Goethals, M., Niedermann, S., Hetzel, R., and Fenton, C.: Determining the impact of faulting on the rate of erosion in a low-relief landscape: A case study using in situ produced ^{21}Ne on active normal faults in the Bishop Tuff, California, Gg~~g~~eomorphology, 103, 401–413, https://doi.org/10.1016/j.geomorph.2008.07.008, 2009.

Gosse, J. C. and Phillips, F. M.: Terrestrial in situ cosmogenic nuclides: theory and application, Quaternary Science Reviews, 20, 1475–1560, https://doi.org/10.1016/S0277-3791(00)00171-2, 2001.

Klemetti, E. W. and Clynne, M. A.: Localized rejuvenation of a crystal mush recorded in zircon temporal and compositional variation at the Lassen Volcanic Center, Northern California, PloS one, 9, e113157, https://doi.org/10.1371/journal.pone.0113157, 2014.

Laabs, B. J., Refsnider, K. A., Munroe, J. S., Mickelson, D. M., Applegate, P. J., Singer, B. S., and Caffee, M. W.: Latest Pleistocene glacial chronology of the Uinta Mountains: support for moisture-driven asynchrony of the last deglaciation, Quaternary Science Reviews, 28, 1171–1187, https://doi.org/10.1016/j.quascirev.2008.12.012, 2009.

Laabs, B. J. C., Licciardi, J. M., Leonard, E. M., Munroe, J. S., and Marchetti, D. W.: Updated cosmogenic chronologies of Pleistocene mountain glaciation in the western United States and associated paleoclimate inferences, Quaternary Science Reviews, 242, 106427, https://doi.org/10.1016/j.quascirev.2020.106427, 2020.

Libarkin, J.C., Quade, J., Chase, C.G., Poths, J. and McIntosh, W.: Measurement of ancient cosmogenic ^{21}Ne in quartz from the 28 Ma Fish Canyon Tuff, Colorado. Chemical Geology, 186(3-4), pp.199-213, https://doi.org/10.1016/S0009-2541(01)00411-9, 2002.

Licciardi, J. M., Clark, P. U., Brook, E. J., Elmore, D., and Sharma, P.: Variable responses of western US glaciers during the last deglaciation, Geology, 32, 81–84, https://doi.org/10.1130/G19868.1, 2004.

Lifton, N., Sato, T., and Dunai, T. J.: Scaling in situ cosmogenic nuclide production rates using analytical approximations to atmospheric cosmic-ray fluxes, Earth and Planetary Science Letters, 386, 149–160, https://doi.org/10.1016/j.epsl.2013.10.052, 2014.

Lifton, N.: Implications of two Holocene time-dependent geomagnetic models for cosmogenic nuclide production rate scaling, Earth and Planetary Science Letters, 433, 257–268, https://doi.org/10.1016/j.epsl.2015.11.006, 2016.

Lisiecki, L. E. and Raymo, M. E.: A Pliocene-Pleistocene stack of 57 globally distributed benthic δ^{18}O records, Paleoceanography, 20, https://doi.org/10.1029/2004PA001071, 2005.

Muffler, L. P. and Clynne, M. A.: Geologic field-trip guide to Lassen Volcanic National Park and vicinity, California, US Geological Survey Scientific Investigations Report 2015-5067, 67 p., https://doi.org/10.3133/sir20155067, 2015.

Niedermann, S., Graf, T., and Marti, K.: Mass spectrometric identification of cosmic-ray-produced neon in terrestrial rocks with multiple neon components, Earth and Planetary Science Letters, 118, 65–73, https://doi.org/10.1016/0012-821X(93)90159-7, 1993.

Niedermann, S.: Cosmic-ray-produced noble gases in terrestrial rocks: dating tools for surface processes, Reviews in mineralogy and geochemistry, 47, 731–784, https://doi.org/10.2138/rmg.2002.47.16, 2002.

O'Hara, D., Karlstrom, L., and Ramsey, D. W.: Time-evolving surface and subsurface signatures of Quaternary volcanism in the Cascades arc, Geology, 48, 1088–1093, https://doi.org/10.1130/G47706.1, 2020.

Palacios, D., Stokes, C. R., Phillips, F. M., Clague, J. J., Alcalá-Reygosa, J., Andrés, N., Angel, I., Blard, P.-H., Briner, J. P., and Hall, B. L.: The deglaciation of the Americas during the Last Glacial Termination, Earth-Science Reviews, 203, 103113, https://doi.org/10.1016/j.earscirev.2020.103113, 2020.

Phillips, W. M., McDonald, E. V., Reneau, S. L., and Poths, J.: Dating soils and alluvium with cosmogenic ^{21}Ne depth profiles: case studies from the Pajarito Plateau, New Mexico, USA, Earth and Planetary Science Letters, 160, 209–223, https://doi.org/10.1016/S0012-821X(98)00076-4, 1998.

Pierce, I. K. D., Wesnousky, S. G., and Owen, L. A.: Terrestrial cosmogenic surface exposure dating of moraines at Lake Tahoe in the Sierra Nevada of California and slip rate estimate for the West Tahoe Fault, Geomorphology, 298, 63–71, https://doi.org/10.1016/j.geomorph.2017.09.030, 2017.

Quirk, B. J., Moore, J. R., Laabs, B. J., Plummer, M. A., and Caffee, M. W.: Latest Pleistocene glacial and climate history of the Wasatch Range, Utah, Quaternary Science Reviews, 238, 106313, https://doi.org/10.1016/j.quascirev.2020.106313, 2020.

Rood, D. H., Burbank, D. W., and Finkel, R. C.: Chronology of glaciations in the Sierra Nevada, California, from ^{10}Be surface exposure dating, Quaternary Science Reviews, 30, 646–661, https://doi.org/10.1016/j.quascirev.2010.12.001, 2011a.

Rood, D. H., Burbank, D. W., and Finkel, R. C.: Spatiotemporal patterns of fault slip rates across the Central Sierra Nevada frontal fault zone, Earth and Planetary Science Letters, 301, 457–468, https://doi.org/10.1016/j.epsl.2010.11.006, 2011b.

Schoenemann, S. W., Bryant, M. M., Larson, W. B., Corbett, L. B., and Bierman, P. R.: A cosmogenic ^{10}Be moraine chronology of arid, alpine Late Pleistocene glaciation in the Pioneer Mountains of Montana, USA, Quaternary Science Reviews, 317, 108283, https://doi.org/10.1016/j.quascirev.2023.108283, 2023.

Schweinsberg, A. D., Briner, J. P., Licciardi, J. M., Shroba, R. R., and Leonard, E. M.: Cosmogenic ^{10}Be exposure dating of Bull Lake and Pinedale moraine sequences in the upper Arkansas River valley, Colorado Rocky Mountains, USA, Quaternary Research, 97, 125–139, https://doi.org/10.1017/qua.2020.21, 2020.

Shakun, J. D., Clark, P. U., He, F., Lifton, N. A., Liu, Z., and Otto-Bliesner, B. L.: Regional and global forcing of glacier retreat during the last deglaciation, Nature Communications, 6, 1–7, https://doi.org/10.1038/ncomms9059, 2015.

Shuster, D. L. and Farley, K. A.: Diffusion kinetics of proton-induced ^{21}Ne, ^{3}He, and ^{4}He in quartz, Geochimica et Cosmochimica Acta, 69, 2349–2359, https://doi.org/10.1016/j.gca.2004.11.002, 2005.

Spector, P. and Balco, G.: Exposure-age data from across Antarctica reveal mid-Miocene establishment of polar desert climate, Geology, 49, 91–95, https://doi.org/10.1130/G47783.1, 2021.

Speth, G. T., Amos, C. B., Amidon, W. H., Balco, G., Meigs, A. J., and Graf, S.: Glacial chronology and slip rate on the west Klamath Lake fault zone, Oregon, GSA Bulletin, 131, 444–460, https://doi.org/10.1130/B31961.1, 2018.

Stone, J. O.: Air pressure and cosmogenic isotope production, Journal of Geophysical Research: Solid Earth, 105, 23753–23759, 2000.

Tulenko, J. P., Lofverstrom, M., and Briner, J. P.: Ice sheet influence on atmospheric circulation explains the patterns of Pleistocene alpine glacier records in North America, Earth and Planetary Science Letters, 534, 116115, https://doi.org/10.1016/j.epsl.2020.116115, 2020.

Turrin, B. D., Christiansen, R. L., Clynne, M. A., Champion, D. E., Gerstel, W. J., Muffler, L. J. P., and Trimble, D. A.: Age of Lassen Peak, California, and implications for the ages of late Pleistocene glaciations in the southern Cascade Range, Geological Society of America Bulletin, 110, 931–945, https://doi.org/10.1130/0016-7606(1998)110<0931:AOLPCA>2.3.CO;2, 1998.

Valentine, G. A., Briner, J. P., van Wyk de Vries, B., Macorps, É., and Gump, D.: 10Be exposure ages for the Late Pleistocene Gour de Tazenat maar (Chaîne des Puys volcanic field, Auvergne, France), Quaternary Geochronology, 50, 8–13, https://doi.org/10.1016/j.quageo.2018.11.002, 2019.

Vermeesch, P., Balco, G., Blard, P.-H., Dunai, T. J., Kober, F., Niedermann, S., Shuster, D. L., Strasky, S., Stuart, F. M., and Wieler, R.: Interlaboratory comparison of cosmogenic ^{21}Ne in quartz, Quaternary Geochronology, 26, 20–28, https://doi.org/10.1016/j.quageo.2012.11.009, 2015.